Adsorption of Radon on Ice Surfaces

B. Eichler,*,† H. P. Zimmermann,† and H. W. Gäggeler†,‡

Paul Scherrer Institut, 5232 Villigen PSI, Switzerland, and Departement für Chemie und Biochemie, Universität Bern, Freiestrasse 3, 3012 Bern, Switzerland

Received: September 10, 1999

The differential molar adsorption enthalpy of radon at zero coverage on the surface of laboratory made ice was determined by the method of low-temperature thermochromatography. Spherical ice particles were prepared as the stationary phase. For the investigation, the short-lived radon isotope ^{220}Rn was used, generated with a ^{232}U-emanation source. Helium served as carrier gas. At a temperature of about 100 K, sharp adsorption peaks of the ^{220}Rn atoms ($\sim 10^8$) were measured. From the measured deposition temperatures the adsorption enthalpy on the surface of the ice spheres was determined as $\Delta H_{ads} = -19.2 \pm 1.6$ kJ/mol. This value is compared with data from the literature for adsorption enthalpies of radon on different solid surfaces. From the estimated solution enthalpy of radon in water and the formation enthalpy of a hypothetical "Rn chlathrate hydrate", it follows that Rn is adsorbed on the ice surface as a free atom. The measured adsorption enthalpy indicates that Rn and ice are not isomorphous and that Rn shows no solubility in the solid phase.

1. Introduction

Radon is a radioactive noble gas, mainly produced in the earth crust from the long-lived primordial radionuclides ^{232}Th and ^{238}U. Of great importance is ^{222}Rn as decay product of ^{238}U since it has a half-life of 3.8 days. Because of the rather long lifetime for this isotope of 5.5 days ($=T_{1/2}/\ln 2$) it emanates to a considerable amount from the uppermost layer of the soil into the atmosphere. The emanation rate depends strongly on the composition of the soil and on humidity as well as changes in atmospheric pressure.[1]

Similar to its lighter noble gas homologues Ar, Kr, and Xe, Rn is able to form chemical compounds (for surveys see refs 2 and 3), but under natural conditions Rn is inert.

All Rn isotopes undergo radioactive decay to nongaseous products. For atmospheric Rn, these products attach to aerosol particles. Radon as well as its decay products are versatile tracers to study transport phenomena in the atmosphere.[4] In addition, atmospheric particles containing Rn decay products are of high relevance to humans since they may be deposited in the respiratory tract, causing high radiation hazards. Therefore, great interest exists in Rn filters. These filters should guarantee removal of Rn, especially in uranium mining, uranium processing, and nuclear fuel processing and refabrication.[3,5−8] With respect to sorption capacity, charcoal surpasses molsieves and silica gel remarkably.[6]

The temperature-dependent adsorption behavior of Rn at solid-state surfaces determines the probability of desorption. As a natural phenomenon the desorption probability of Rn from the surface of cosmic objects (e.g., from the surface of the moon) has also been investigated.[9]

Knowledge of the adsorption behavior of radon on solid surfaces is required to model its distribution processes. Despite the fact that large areas of the earth surface are covered by ice, little is known about adsorption of radon on ice. Knowledge of this process is important for, e.g., application of the radon decay product ^{210}Pb ($T_{1/2} = 22$ y) for dating purposes.

In this work, the adsorption behavior of radon on ice surfaces is investigated by low-temperature gas adsorption chromatography in form of thermochromatography.[10]

2. Experimental Section

Thermochromatography is a well-known gas chromatographic technique in which a stationary negative temperature gradient (in the direction of the carrier gas flow) is maintained along a chromatographic column. For a given time, the species of interest are injected into the chromatography column which is usually filled with a stationary phase of interest (e.g., ice spheres). After the experiment, the deposition zone of the species and from this the deposition temperature is deduced. From the measured deposition temperature the adsorption enthalpy of the species on the surface of the stationary phase may be calculated. For a description of this technique we refer to refs 10−12. In the following, only some specific problems encountered in the preparation and handling of chromatography columns with ice as the stationary phase are discussed.

Deionized water was used for the preparation of spherical ice particles. The water was dripped at a defined rate out of a Teflon capillary (i.d. 0.5 mm) into a Dewar filled with liquid nitrogen. The end of the capillary was connected to an electrical vibrator to guarantee reproducible formation of small droplets. Obviously, the droplets freeze at the very moment of contact with liquid nitrogen, conserving their shape. They showed a smooth glossy surface. The mass of a single sphere was determined to be 0.7 mg. After production of sufficient ice spheres, the liquid nitrogen was decanted. The particles could then easily be filled in columns. All further manipulations such as the preparation of the columns and the storage were performed in a cold room kept at −20 °C. We assume that during the fast solidification process of liquid water droplets at liquid nitrogen temperature, amorphous ice (I_a) or cubic ice (I_c) is formed. During storage at −20 °C both ice phases (modifications) most likely transform into hexagonal ice (I_h). This transformation takes places even at −120 °C during 2−3 days.[49]

Teflon (PTFE) tubes with 5 mm i.d. were used as columns.

† Paul Scherrer Institut.
‡ Universität Bern.

10.1021/jp9932158 CCC: $19.00
Published on Web 03/21/2000

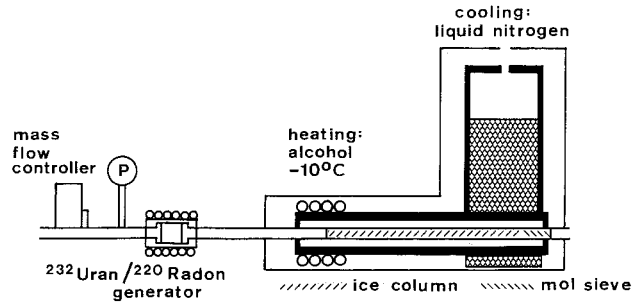

Figure 1. Scheme of the experimental setup.

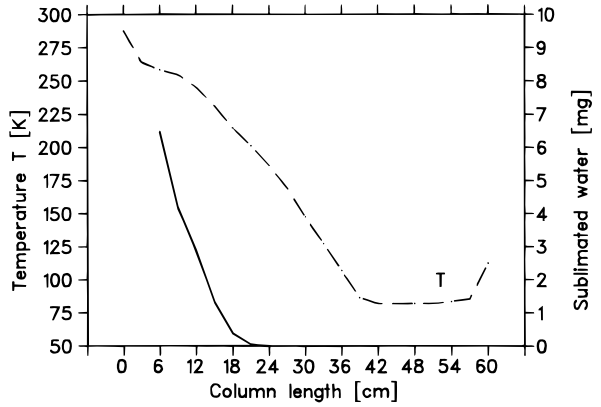

Figure 2. Temperature profile in the column and mass transport of water at a He gas flow rate of 100 mL/min during the experiment (duration 2 h).

The ice spheres were fixed with quartz-wool plugs inserted into the tubes at both ends. One end of the tube was filled with molsieve 5A as sorbent for gaseous species which might break through the stationary phase during the experiment (see Figure 1). Prior to an experimental investigation the columns were pretreated for about 100 h at −20 °C. During that time an equilibrium condition of the solid surface was established via water vapor transport. Neither changes of the shape or surface nor any formation of open porosity was observed visually.

The temperature gradient along the column was generated by the setup shown in Figure 1. As a heat conductor a brass tube with a wall thickness of 2 mm and an inner diameter of 8 mm was used. The "hot" end of the tube was kept at −10 °C by a flux of alcohol, passing through a cryostat. The "cold" end was placed at the bottom of a metal container filled with liquid nitrogen. The entire setup was heavily isolated with Styrofoam.

The temperature profile was measured in an empty column with flowing carrier gas. It was assumed that the temperature profile of the empty column resembles very much that of the filled column due to the high heat conductivity of the He-carrier gas and the turbulence of the gas in the stationary phase.

The temperature profile and the calculated mass transport of water for representative experimental conditions in direction of decreasing temperature are displayed in Figure 2. The values are based on equilibrium partial pressure values of water over the ice surface.[13,14] In the region of radon deposition (see Figure 3) the partial pressure of water is so low that a perceptible transport of water may be excluded. Therefore, it can be assumed in good approximation that in that region the surface is not significantly increased during the experiment.

The adsorption chromatographic investigations in the ice columns were performed with ^{220}Rn. The ^{220}Rn, as emanation of a ^{232}U source, was injected into the He-carrier gas. The source

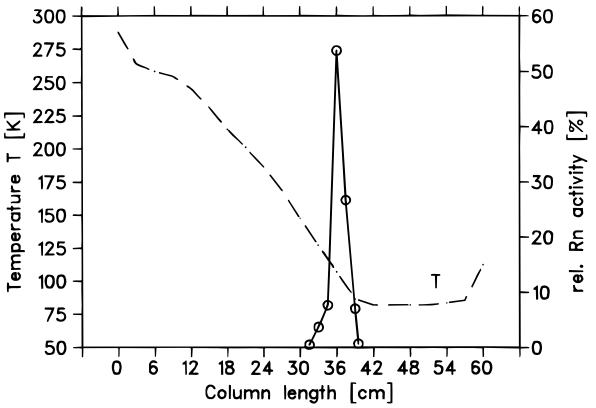

Figure 3. Distribution of the ^{220}Rn decay products along the ice column at a He gas flow rate of 100 mL/min.

TABLE 1: Parameters of Thermochromatographic Experiments

symbol	explanations	values and units
τ_0	period of oscillation of the adsorbat vertically to the surface	3×10^{-13} s
R	gas constant	8.31 J/(mol K)
T_0	standard temperature	298 K
c°_{gas}	standard concentration particles/volume	cm^{-3}
c°_{ads}	standard concentration particles/surface area	cm^{-2}
M	molecular weight	220 g
υ_0	gas flow rate	10−200 cm^3/min
t_r	retention time	1.34 min
ΔH°	standard enthalpy of the respective reaction	kJ/mol
ΔS°	standard entropy of the respective reaction	J/(mol K)
T_D	deposition temperature	K
$Ei^*(x)$	integral exponential function of x, $x = \Delta H_{ads}/RT_D$ or $\Delta H_{ads}/RT_S$ in eq 1; see also Figure 4 and ref 11	
T_s	starting temperature	263 K
g	temperature gradient	5.5 K cm^{-1}
a	surface area per unit of column length	8.5 cm^2/cm
f	factor $= [c^\circ_{ads}]/[c^\circ_{gas}] = cm^3/cm^2$	1 cm

was prepared by evaporation of a solution of ^{232}U in nitric acid on quartz powder. To achieve constant and high ^{220}Rn emanation during the experiment the source was kept at 300 °C.

During the chromatographic transport in the ice column ^{220}Rn decays with a half-life of 55.6 s. The Rn produces nonvolatile decay products: ^{216}Po (0.15 s) and the longer lived isotopes ^{212}Pb (10.6 h) and ^{212}Bi (60.6 min). All these progenies immediately stick to the ice surface. Detection of the activity of the long-lived products, mainly ^{212}Pb, after an experiment can therefore be used as tracer for the position at which ^{220}Rn decayed. With such an approach the chromatographic retention time t_r equals the lifetime τ of ^{220}Rn (1.34 min) which is much shorter than a typical duration of an experiment (about 2 h).

After the column is introduced in the temperature gradient brass tube, the carrier gas was switched on until the temperature equilibrium was reached. Then the ^{220}Rn generator was plugged in the He-carrier gas stream at the "hot" side. All experimental parameters are listed in Table 1.

After the experiment (120 min) the column was removed from the low-temperature end of the gradient tube. Both ends were sealed with silicone plugs. The column was then positioned in a shallow U-shaped container filled with liquid nitrogen.

In this frozen state the activity distribution along the column was measured in 1.5 cm increments with a Geiger−Müller counter in combination with a lead collimator (see Figure 3 for

TABLE 2: Flow Rates and Experimental Results

expt	gas flow rate (cm^3/min)	exptl deposition temp T_D[a] (K)	calcd (eq 2) ads entropy ΔS_{ads} (J/(mol K))	deduced (eq 1) ads enthalpy ΔH_{ads}[a] (kJ/mol)
1	10	110	−170.3	−18.1
2	10	116	−170.1	−19.0
3	20	115	−170.1	−19.6
4	50	112	−170.2	−20.0
5	50	115	−170.2	−19.3
6	100	107	−170.1	−19.8
7	100	110	−170.3	−20.3
8	200	95	−170.9	−18.2
9	200	98	−170.8	−18.7

[a] Typical errors (1σ): $\Delta T_D = \pm 5$ K; $\Delta H_{ads} = \pm 0.7$ kJ/mol.

an example). The deposition temperature T_D of ^{220}Rn is defined as the temperature corresponding to the peak maximum.

3. Results and Discussion

3.1. Measured Deposition Peaks at Different Gas Flow Rates. Table 2 summarizes the deposition temperatures T_D of the peaks measured in nine experiments performed at different gas flow rates. The errors represent the standard deviations of the peaks. They therefore do not include systematic errors.

Despite the small number of Rn atoms ($\sim 10^8$) used for each experimental study, a well-defined peak is observed. This fact is worth mentioning because at the low temperatures which are required for the adsorption of Rn, the formation of a deposition peak is not a priori expected. Diffusion coefficients decrease with temperature and could therefore prevent a peak formation.

In the molsieve section only small traces of the activity were found. This proves that ^{220}Rn decayed nearly completely in the ice column. Also, the formation of sharp adsorption peaks indicates that the decay products (Po, Pb, Bi, Tl) are preserved at the location of their formation, as expected.

3.2. Determination of the Adsorption Enthalpy. From the experimentally determined deposition temperatures the adsorption enthalpy can be calculated with[11]

$$\frac{t_r \upsilon_0 g}{a T_0 f \exp(\Delta S^0_{ads}/R)} = Ei^*\left(\frac{-\Delta H^0_{ads}}{RT_D}\right) - Ei^*\left(\frac{-\Delta H^0_{ads}}{RT_s}\right) \quad (1)$$

with

$$\Delta S^0_{ads} = R \ln\left[\frac{c^0_{gas}}{c^0_{ads}} \tau_0 \left(\frac{RT_D}{2\pi M}\right)^{1/2}\right] + R/2 \quad (2)$$

All symbols are explained in Table 1 as well as some experimental parameters.

To obtain the adsorption enthalpy from the measured data (see Table 2), the adsorption entropy must first be calculated. This can be performed with the model of mobile adsorption[15] assuming that the adsorption entropy may be calculated for the temperature which corresponds to T_D since the Rn atoms stay during most of the time near the deposition position.

The period of oscillation τ_0 necessary to calculate the entropy of adsorption was derived from the vibrational frequency ν of the solid state of ice. Since no experimental data exist for τ_0 or ν, the period of oscillation τ_0 was estimated with data from ref 49 applying the relations from Madelung and Einstein ($\tau_0 = 3.1 \times 10^{-13}$ s), Lindemann ($\tau_0 = 2.5 \times 10^{-13}$ s) and Debye ($\tau_0 = 3.4 \times 10^{-13}$ s).[16] A rounded value of 3×10^{-13} s was used for further calculations.

TABLE 3: Adsorption Enthalpies of Radon on Solid State Surfaces

adsorbent	$-\Delta H_{ads}$ (kJ/mol)	carrier gas	temp (K)	ref
silica gel	37.7	air or argon	298	17
	28.7	air	204−303	18
charcoal	35.6	hydrogen	293−353	19
	32.7	nitrogen	293−353	19
	30.0	air	293−303	19
	28.9	air	273−323	20
	31.4	air	204−303	18
	35.4 ± 5.2	helium	193−373	20
palladium	37.0 ± 4.0	hydrogen	168	21
ice	19.2 ± 1.6	helium	90−115	this work

TABLE 4: Mean Values of Adsorption Enthalpies of Noble Gases on Different Adsorbents from the Literature[a]

noble gas	$-\Delta H_{ads}$ (kJ/mol) charcoal	silica gel	molsieve	TiO_2
He	1.7 ± 0.7 (22−24)			
Ne	5.4 ± 0.9 (23−25)			6.4 (37)
Ar	11.2 ± 3.7 (22−31)	13.2 ± 5.4 (17, 26)	13.9 ± 4.2 (6, 27, 29, 34, 35)	7.2 (28)
Kr	16.1 ± 3.1 (22, 23, 25, 26, 28−32)		17.0 ± 4.3 (27, 31, 34, 36)	13.3 ± 0.5 (30)
Xe	24.3 ± 7.8 (22, 25, 26, 32, 33)		26.6 ± 5.4 (31, 36)	19.8 (10)
Rn	35.8 ± 7.0 (5, 19, 20)	33.2 ± 4 (17, 18)		

[a] The adsorption enthalpies were determined by isothermal gas chromatography (refs 25−28, 35), from adsorption isotherm or isostere (dynamic: refs 5, 18, 19, 36; static: refs 20, 34), by calorimetry (ref 37), and from a literature survey (refs 6, 22−24, 30−32).

Averaging all unweighted experimental values yields:

$$\Delta H_{ads} = -19.2 \pm 1.6 \text{ kJ/mol} \qquad (2\,\sigma \text{ uncertainty})$$

Under the condition of a temperature-independent adsorption enthalpy, and using the calculated entropy (eq 2), the dimensionless equilibrium constant K_{ads} of the adsorption reaction for temperatures close to the deposition temperature is given by

$$\ln K_{ads} = -\frac{(\Delta H_{ads} - T \cdot \Delta S_{ads})}{RT} \quad (3)$$

resulting in

$$\log K_{ads} = (1004 \pm 92)/T - 8.9 \pm 0.1 \quad (4)$$

3.3. Comparison with Adsorption Enthalpies on Different Adsorbents. Literature values for the adsorption behavior of radon on ice surfaces are not available. Therefore, only thermochemical literature data for other radon-adsorbent combinations can be used for comparison (Table 3). All values relate to very small degrees of coverage. The adsorption enthalpy of radon on ice surfaces is clearly lower than the values measured with any other adsorbent.

The most important interactions between radon and solid-state surfaces base on dispersion forces. By their nature, such forces are similar to the interaction between radon atoms in a condensed state. To demonstrate this assumption the adsorption enthalpies of noble gases on different sorbent materials (Table 4) are plotted in Figure 4 as a function of the sublimation enthalpies of the noble gases. Obviously, there is a proportionality between the two values for a given sorbent.

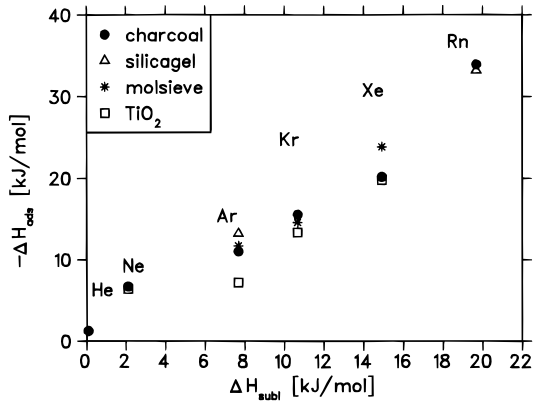

Figure 4. Adsorption enthalpies of noble gases on surfaces of solid adsorbents (see Table 4) versus their sublimation enthalpies.

TABLE 5: Atomic or Molecular Radii, Ionization Potentials, and Polarizability of the Atoms of Radon and Carbon and the Water Molecule

	Rn	C	H_2O
radius r (10^{-9} m)	0.18[a]	0.071[b]	0.14[a]
ionization potentials I (eV)	10.75[13]	11.26[13]	12.61[41]
polarizability α (10^{-30} m^3)	6.14 (eq 7)	1.76[39]	1.44[39,52]
$g^{\ddagger} = (\epsilon_0 - 1)/(\epsilon_0 + 1)$[39]		1.0	0.99[c]
molar polarization P_M (10^{-6} m^3)	15.49 (eq 8)		

[a] Derived from the van der Waals constant b. [b] Graphite[42] [c] Value for dielectric constant ϵ_0 from ref 51.

In the following, an estimate is made on the dispersion energies between Rn and graphite as well as Rn and ice. Graphite is taken as example, since for this sorbent reliable experimental data exist (see Table 3). The dispersion energies W between two particles can be calculated with[38]

$$W = -\frac{3}{2}\frac{\alpha_1\alpha_2}{(r_1 + r_2)^6}\left(\frac{E_1E_2}{E_1 + E_2}\right) \tag{5}$$

with $E_{1,2} = 1.57I_{1,2}$, and W the dispersion energy, $\alpha_{1,2}$ polarizability of the particles, $r_1 + r_2$ distance of the centers of the particles, $E_{1,2}$ average dipole transition energies, and $I_{1,2}$ first ionization potentials.

For a comparison of the interaction between radon and different adsorbents, the ratio of the dispersion energies can be derived from

$$\frac{W_C}{W_{H_2O}} = \frac{\alpha_C(r_{Rn} + r_{H_2O})^6}{\alpha_{H_2O}(r_{Rn} + r_C)^6}\frac{I_CI_{Rn} + I_CI_{H_2O}}{I_{H_2O}I_{Rn} + I_CI_{H_2O}} \tag{6}$$

This ratio was calculated with the data for charcoal (C) and water (H_2O) compiled in Table 5.

The polarizability of radon was extrapolated from an empirical correlation of the polarizability of the noble gases[39,40] with their sublimation enthalpies[13] with a polynomial expansion:

$$\alpha = 0.0096\Delta H_{subl}{}^2 + 0.1147\Delta H_{subl} + 0.1624 \tag{7}$$

With $\Delta H_{subl} = 19.69$ kJ/mol,[13] $\alpha = (6.1428 \pm 0.0023) \times 10^{-30}$ m^3 is obtained.

Polarizability α and molar polarization P_M are connected by

$$P_M = {}^4/_3\pi N_L\alpha \tag{8}$$

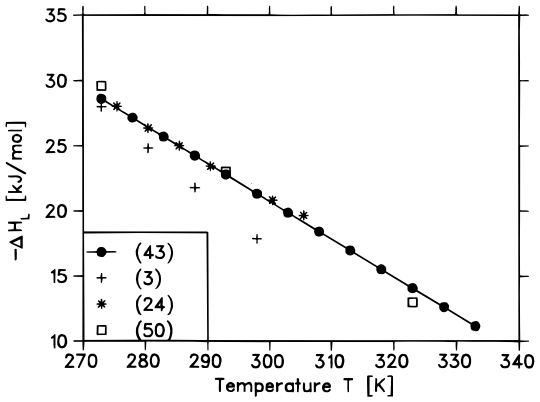

Figure 5. Solution enthalpies of radon in water at different temperatures from refs 3, 24, 43, 50. The linear regression fits only the data of ref 43.

With these data the following ratio is obtained:

$$W_C/W_{H_2O} = 4.6$$

According to this ratio of the dispersion energies, it can be expected that the absolute value of the adsorption enthalpy of radon on ice is much smaller than on charcoal. The experimental result is in agreement with this prediction.

The energy of the van der Waals interaction of polarizable atoms with a surface of a dielectric material or a metal can be estimated with[39]

$$W = \frac{\alpha_1 g^{\ddagger}}{8(r_1 + r_2)^3}\frac{E_1E_2}{(E_1 + E_2)} \tag{9}$$

Again utilizing data from Table 5 we obtain for the "adsorption energies" of radon on

charcoal $W_{Rn-C} = 36.2$ kJ/mol

and on

ice $W_{Rn-ice} = 18.9$ kJ/mol

These values agree well with experimental data (see Table 3).

3.4. Interaction of Radon with Water and Ice in Bulk Phases. Finally, we discuss the interaction of Rn with water and ice in bulk phases. Figure 5 displays the temperature dependence of the solution enthalpy of radon in water. The solution enthalpy $-\Delta H_L(T)$ increases with decreasing temperature according to[43]

$$-\Delta H_L(T) = -0.291T + 108.053 \tag{10}$$

The standard enthalpy of solution is $\Delta H^\circ_L(298) = -22.79$ kJ/mol and at 0 °C $\Delta H^\circ_L(273) = -28.61$ kJ/mol.[43]

During the solution process of radon a reorientation of the water molecules in the neighborhood of the nonpolar atom takes place.[44] A chlathrate-like cage is formed around the Rn atom. The strength of the hydrogen bonds increase slightly. The formation of the cage around the Rn atom contributes to the enthalpy of solution.

The interaction of the polarizable radon with the solvent water is much stronger than the measured adsorption enthalpy of Rn on ice. Therefore, in the adsorbed state on ice surfaces radon is not completely surrounded with water molecules.

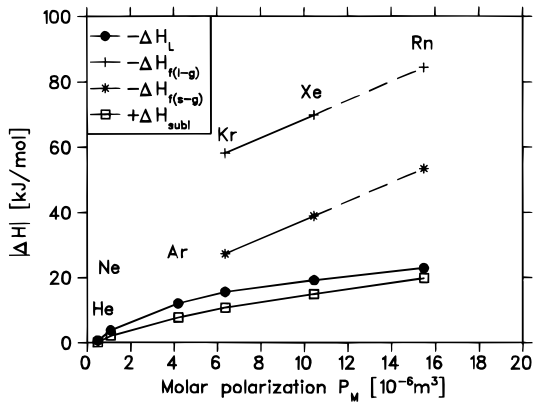

Figure 6. Correlation of the sublimation enthalpies (ΔH_{subl}) and the solution enthalpies (ΔH_L)[13,44] as well as the formation enthalpies (ΔH_f) of the chlathrates[22,47] of the noble gases as a function of their molar polarization. ΔH_f for Rn: extrapolated value; l-g: liquid water−$Rn_{(g)}$; s-g: ice−$Rn_{(g)}$.

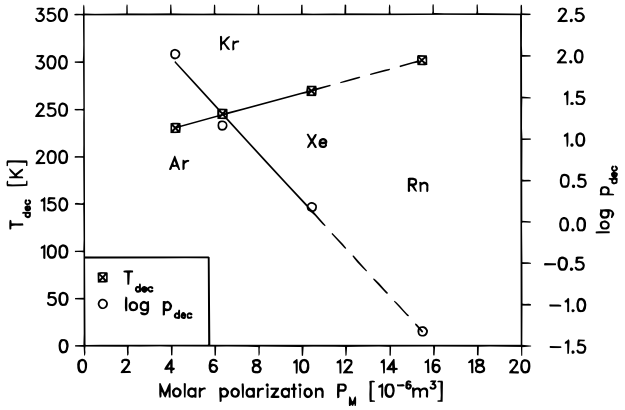

Figure 7. Correlation of the decomposition temperatures at a pressure of 1 atm as well as the decomposition pressures at a temperature of 273 K of the chlathrates of the noble gases[22,47] as a function of their molar polarization (Rn: extrapolated values).

A long known[45,46] but poorly investigated compound is radon chlathrate hydrate. Noble gas compounds of this type are formed when Ar, Kr, or Xe is passed through water under high pressure at low temperatures. Their structure can be described as occlusion compounds with $X_8 \cdot H_{46}O_{23}$ units, with X being a noble gas atom. For Rn only mixed hydrates with other gases (SO_2, H_2S, etc.) are known. Probably single atoms are not able to form such chlathrates. Nikitin[45] described the formation of the chlathrates with SO_2 as isomorphous cocrystallization of the single chlathrates with the stoichiometric constitution: $X \cdot H_{12}O_6$. According to more recent models[22,47] the cages are filled with help gases.

Extrapolated data for the stability of a hypothetical radon chlathrate hydrate from literature data of formation enthalpies, decomposition pressures, and temperatures as functions of the molar polarization are shown in Figures 6 and 7. The linear extrapolation in Figure 6 results in upper limits of the formation enthalpies. The formation enthalpy of a hypothetical radon chlathrate compound, related to 1 mol Rn surpasses the measured adsorption enthalpy of about 20 kJ/mol considerably.

3.5. Influence of the Adsorbent Properties. The differential molar adsorption enthalpy at zero coverage may be calculated from the desublimation enthalpy (ΔH_{desubl}), the differential molar solution enthalpy of the solid adsorbat in the pure solid adsorbent ($\overline{\Delta H_L}$), and the enthalpy of vacancy formation (ΔH_{VV}):[48]

$$\overline{\Delta H}_{ads} = \Delta H_{desubl} + 0.6\left(\overline{\Delta H}_L - \frac{V_A}{V_B}\cdot\Delta H_{VV}\right) \qquad (11)$$

V_A/V_B is the ratio of the volumes of the atoms of the adsorbate and the molecules of the adsorbent, respectively.

Since the measured adsorption enthalpy of radon on ice approximately corresponds to the desublimation enthalpy, the differential molar enthalpy of solution of solid radon in solid ice must be equal to the displacement enthalpy $(V_A/V_B)\Delta H_{VV}$, which is necessary for the uptake of 1 mol radon in ice of normal structure (ice I). With $\Delta H_{VV} = 51$ kJ/mol[49] it follows that $\overline{\Delta H}_L = +105$ kJ/mol.

The sign and order of magnitude of this value are in agreement with the fact that solid radon and ice are not isomorphous and not soluble in each other in the solid phase.

4. Conclusions

1. Gas adsorption chromatographic studies are well suited to study the behavior of trace gases with spherical ice particles down to liquid nitrogen temperature. Under such conditions, thermochromatographic experiments allow the determination of adsorption enthalpies in the range of $15 < -\Delta H_{ads} < 60$ kJ/mol.

2. A comparison of the experimentally determined adsorption enthalpy of radon on ice of -19.2 ± 1.6 kJ/mol with the adsorption enthalpies of radon on other solid state surfaces, the solution enthalpy of radon in water, and the formation enthalpy of a hypothetical radon chlathrate hydrate shows that with a high probability radon is adsorbed as a free atom on the ice surface and is not fully coordinated by water dipoles.

3. On the basis of the calculated temperature-dependent adsorption entropy and the experimental adsorption enthalpy, assumed to be temperature independent, the equilibrium constant of the adsorption reaction can be given for a small temperature range around the deposition temperature in a thermochromatographic column.

References and Notes

(1) Clements, W. E.; Wilening, M. H. *J. Geophys. Res.* **1974**, *79*, 5025.
(2) Stein, L. *Radiochim. Acta* **1983**, *32*, 163.
(3) Weigel, F. *Chem. Z.* **1978**, *102*, 287.
(4) Sanak, J. Radon-222 as an atmospheric tracer; In *Isotopes of Noble Gases as Tracers in Environmental Studies*; Proceedings of a Consultants Meeting, Vienna, 29 May−2 June 1989; IAEA: Vienna, 1992.
(5) Strong, K. P.; Levins, D. M. *Dynamic Adsorption of Radon on Activated Carbon*; Nuclear Air Cleaning Conference, Boston, MA, Aug 1978; Conf-780819-P2, p 627.15.
(6) Ackley, R. D. *Removal of Radon-220 from HTGR fuel reprocessing and refabrication off-gas streams by adsorption (based on a literature survey)*; ORNL-TM-4883, 1975.
(7) Hohorst, F. A. *Containment of 220-Radon via adsorption on molecular sieves for HTGR-OGCS*; Report ICP-1114, Idaho National Engineering Lab, Idaho Falls, ID, 1977.
(8) Hirsch, P. M.; Higuchi, K. Y.; Abraham, L. *Carbon Dioxide-Krypton Separation and Radon Removal from Nuclear-Fuel-Reprocessing Off-Gas Streams*; General Atomic Co., 1982; GA-A 16809.
(9) Friesen, L. J. *Radon diffusion and migration at low pressures in the laboratory, and on the Moon*; Ph.D. Thesis, Rice University, Houston, TX, 1974; University Microfilms Order No. 74-21, 270.
(10) Eichler, B.; Baltensperger, U.; Ammann, M.; Jost, D. T.; Gäggeler, H. W.; Türler, A. *Radiochim. Acta* **1995**, *68*, 41.
(11) Eichler, B.; Zvara, I. *Radiochim. Acta* **1982**, *30*, 233.
(12) Eichler, B.; Zude, F.; Fan, W.; Trautmann, N.; Herrmann, G. *Radiochim. Acta* **1993**, 61.
(13) Effimov, A. J. *Svoistva neorganiceskikh soedinenie*; Izd. Khimiya: Leningrad, 1983.
(14) Jansco, G.; Pupezin, J.; Van Hook, W. A. *J. Phys. Chem.* **1970**, *64*, 2984.
(15) de Boer, H. J. *The Dynamical Character of Adsorption*; Clarendon Press: Oxford, UK, 1953.

(16) Schwabe, K. *Physikalische Chemie*; Akademieverlag: Berlin, 1973; p 84.
(17) Burtt, B. P.; Kurbatov, J. D. *J. Am. Chem. Soc*. **1948**, *70*, 2278.
(18) Gübeli, O.; Stammbach, K. *Helv. Chim. Acta* **1951**, *34*, 1257.
(19) Gübeli, O.; Störi, M. *Helv. Chimica Acta* **1954**, *37*, 2224.
(20) Kazankin, Yu. N.; Trofimov, A. M.; Mikhailova, L. K. *Radiokhimiya* **1978**, *20* (3), 426.
(21) Eichler, B.; Kim Son Chun. *Isotopenpraxis* **1985**, *21*, 180.
(22) Barlett, N. The Chemistry of Kr, Xe and Rn. In *Comprehensive Inorganic Chemistry*; Bailor, J. C., et al., Eds.; Pergamon Press: New York, 1973; p 233.
(23) Cook, G. A. *Argon, Helium and the Rare Gases*; Interscience Publishers: New York, 1961.
(24) *Gmelins Handbuch der Anorganischen Chemie*, 8.Auflage; Edelgase, Verlag Chemie: Weinheim, Germany, 1926.
(25) Cremer, E. *Z. Anal. Chem.* **1959**, *170*, 219.
(26) Kiselev, V. *Fiziko-khimiceskoje primenenie gasovoi chromatografii*; Izd. Khimiya: Moscow, 1973; p 25.
(27) Greene, S. A.; Pust, M. *J. Phys. Chem*. **1958**, *62*, 55.
(28) Ross, S.; Olivier, J. P. *J. Phys. Chem*. **1961**, *65*, 608.
(29) Barrer, R. M.; Rees, L. V. C. *Trans. Faraday Soc.* **1961**, *57*, 999.
(30) Flood, E. A. *The Solid-Gas Interface*; Marcel Dekker: New York, 1967; Vol. I.
(31) Breck, D. W. *Zeolite Molecular Sieves*; John Wiley & Sons: New York, 1974.
(32) Ross, S.; Olivier, J. P. *J. Phys. Chem*. **1961**, *65*, 608.
(33) Cochran, H.; Walker, P. L.; Diethorn, W. S.; Fridman, H. C. *J. Colloid Interface Sci*. **1967**, *24*, 405.
(34) Seewald, H. *Technisch verfügbare Adsorbentien*; Vertragsveröffentlichung; Haus Technik: Berlin, Germany, 1977; Vol. 404, p 24.
(35) Kiseljev, A. V. *Zh. Fiz. Khim*. **1967**, *41*, 2470.
(36) Kitani, S.; Takata, J. *J. Nucl. Sci. Technol*. **1965**, *2*, 405.
(37) Tykodi, R. J.; Aston, J. G.; Schreiner, G. D. L. *J. Am. Chem. Soc*. **1955**, *77*, 2168.
(38) Pauling, L. *Science* **1961**, *134*, No. 3471, 15.
(39) *CRC Handbook of Chemistry and Physics*, 76th ed.; Lide, D. R., Frederikse, H. P. R., Eds.; CRC Press: New York, 1996; Table 10-194.
(40) Radzig, A. A. *Spravocnik po atomnoi i molekularnoi fizike*; Atomizdat: Moscow, 1980.
(41) Gurvic, L. V. *Energija Razriva khimiceskikh Svjazei*; Izd. Nauka: Moscow, 1974.
(42) Halla, F. *Kristallchemie und Kristallphysik metallischer Werkstoffe*; Barth-Verlag: Leipzig, 1957; p 35.
(43) Young, C. L.; Battino, R.; Clever, H. L. The Solubility of Gases in Liquids. In *Solubility Data Series, Vol. 2; Krypton, Xenon and Radon-Gas Solubility*; Clever, H. L., Ed.; Pergamon Press: New York, 1978; p 228.
(44) Smith, S. P.; Kennedy, B. M. *Geochim. Cosmochim. Acta* **1983**, *47*, 503.
(45) Nikitin, B. A. *Z. Anorg. Allg. Chem*. **1936**, *227*, 81.
(46) Nikitin, B. A. *Nature* **1937**, *140*, 643.
(47) Jeffrey, G. A.; McMullan, R. K. The Chlathrate Hydrates. In *Progress in Inorganic Chemistry*; Cotton, F. A., Ed.; Interscience: New York, 1967; p 43.
(48) Eichler, B. *Bestimmung der Adsorptionswärme gasförmiger Metalle auf festen Metalloberflächen bei Null-Bedeckung* (Empirisches Modell); Report ZfK-396, Rossendorf, 1979.
(49) Hobbs, P. V. *Ice Physics*; Clarendon Press: Oxford, UK, 1974; p 388.
(50) Beggerow, G. *Landolt-Börnstein, Neue Serie, Gruppe IV: Makroskopische und technische Eigenschaften der Materie, Band 2. Mischungs- und Lösungswärmen*; Springer-Verlag: Heidelberg, Germany, 1976; p 109.
(51) *Gmelins Handbuch der Anorganischen Chemie*, 8.Auflage; Sauerstoff, Syst. No. 3; Verlag Chemie: Weinheim, Germany, 1963; p 1586.
(52) Barrow, G. M. *Physical Chemistry*; McGraw-Hill: New York, 1973; p 404.